Glutathione in the noncanonical biosynthesis of teredinibactins

Youjung Sung, Bailey W. Miller, and Eric W. Schmidt

Department of Medicinal Chemistry, University of Utah, Salt Lake City, UT USA 84112

ABSTRACT: Teredinibactins are ß-resorcyclic thiazoline dipeptides synthesized by *Teredinibacter turnerae* T7901, a bacterial symbiont of shipworms in the sea. Through feeding studies, we show that the thiazoline moiety is made from glutathione and its metabolites in a noncanonical peptide azoline pathway. Mimicking the biosynthetic reaction, we synthesized both natural and unnatural teredinibactins. The results expand the scope of biological and chemical approaches to aromatic azoline conjugates.

Thiazoline and related motifs are important functional groups in bioactive natural products and pharmaceuticals.[1] The biosynthetic routes have been widely studied,[2] yielding tools for biotechnology,[3] while synthetic methods have contributed to diverse fields from orthogonal protein labeling[4] to pharmaceutical chemistry.[1] Peptide thiazolines are typically biosynthesized from cysteine by the action of nonribosomal peptide synthetases (NRPSs)[5] or as ribosomally synthesized and posttranslationally modified peptides (RiPPs).[6] For example, yersiniabactin-type siderophores are formed through the NRPS-catalyzed condensation of salicylate with cysteine, which is then heterocyclized to thiazoline (Figure 1).[7] Metal-binding teredinibactins are similar to yersinibactin, containing a ß-resorcyclic moiety linked to thiazoline derived from cysteine and glycine.[8] However, in seeking the teredinibactin biosynthetic gene cluster (BGC) in the producing gammaproteobacterium *Teredinibacter turnerae* T7901,[9] we could not identify any candidate thiazoline-producing NRPSs, nor could we identify potential biosynthetic genes from any other known azoline biosynthetic pathway. This implied a potentially noncanonical route to thiazoline biosynthesis.

T. turnerae lives in the gills of shipworms in the oceans, where it secretes cellulases to help the shipworms digest wood and produces several potent antibiotics.[10] To the best of our knowledge, teredinibactin-like compounds have not been found elsewhere, but Cys-Gly azoline natural products have been described in several bacterial species and in the plant *Arabidopsis thaliana*. In bacteria, the glutathione metabolic product Cys-Gly is thought to possibly non-enzymatically react with an indole-pyruvate derivative to yield indolokines.[11] In *A. thaliana*, related compounds are made from glutathione, which is added enzymatically to a nitrile and then proteolyzed to form the azoline.[12, 13] Similarly, Cys, Cys-Gly, and glutathione are non-enzymatically added to the nitrile electrophile in the FDA-approved drug, vidagliptin.[14] We therefore reasoned that Cys-Gly might directly couple with an electrophilic aromatic species, possibly a nitrile.

While glutathione and related metabolites are universal,[15] ß-resorcyclic acids have rarely been reported from bacteria. Therefore, we aimed to determine whether the compounds were truly natural products, or whether they originated in an electrophile contaminant that might be present in the fermentation conditions. *T. turnerae* grows in minimal media (shipworm basal medium, SBM)[16] with addition of carbon sources such as sucrose, glucose, and cellulose. While some strains fix nitrogen, an ammonium nitrogen source is efficiently used by *T. turnerae*. When we grew *T. turnerae* with U-^{13}C-glucose as the sole carbon source, all 12 carbons present in teredinibactin A (**1**) and dechloroteredinibactin (**2**) were fully labeled by ^{13}C (Figure 2A, bottom panel). In addition, when grown with ^{15}N-ammonium chloride, *T. turnerae* produced **1** and **2** in which the two nitrogens were completely labeled with ^{15}N (Figure 2B, top panel). Therefore, teredinibactins are true metabolic products of *T. turnerae*.

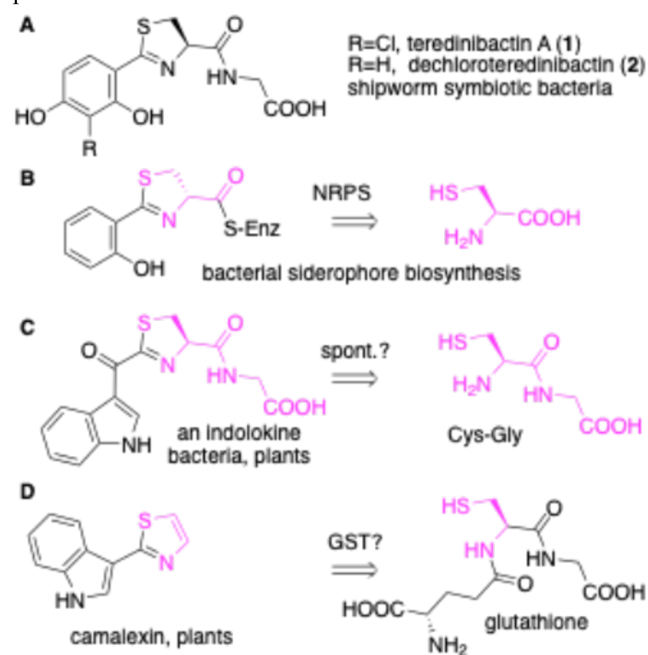

Figure 1. Teredinibactins and related metabolites from bacteria and plants. A) The most abundant teredinibactin natural products. B) Siderophores such as yersiniabactin are made from cysteine via a nonribosomal peptide synthetase (NRPS) enzyme. C) Indolokines might originate from a spontaneous reaction between Cys-Gly and an indole derivative, at least in bacteria. D) Camalexin is made from an indole nitrile and glutathione, likely by the action of a glutathione *S*-transferase (GST).

https://doi.org/10.26434/chemrxiv-2024-ph6m0 **ORCID:** https://orcid.org/0000-0003-3204-3235 Content not peer-reviewed by ChemRxiv. **License:** CC BY-NC-ND 4.0

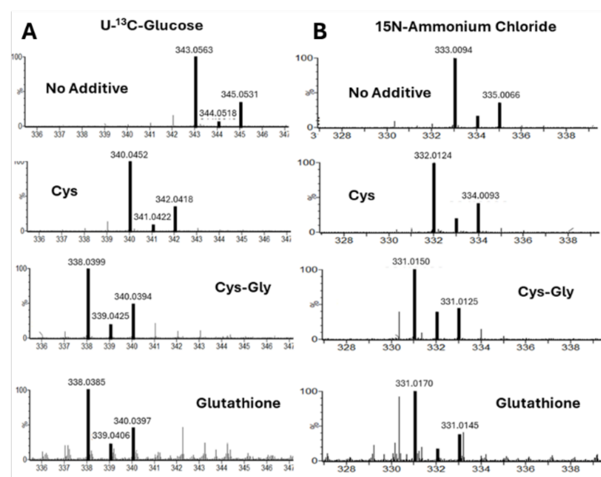

Figure 2. Feeding study with glutathione and derivatives. Each panel shows the mass spectrum of **1** grown in the presence of (**A**) U-^{13}C-glucose and (**B**) ^{15}N-ammonium chloride. The added unlabeled derivative is written in the corresponding panel, and the mass spectra show robust incorporation of intact glutathione, Cys-Gly, and Cys.

To determine the origin of the Cys-Gly dipeptide, we used Puri's inverse labeling method.[17] *T. turnerae* was grown with U-^{13}C-glucose or ^{15}N-ammonium chloride as the sole carbon or nitrogen source, respectively. In separate experiments, unlabeled Cys, Cys-Gly, or glutathione (each at 5 mM) were added to the culture. These experiments were repeated a total of three times. Glutathione was the most difficult to observe because at 5 mM glutathione slowed the growth of *T. turnerae* and depressed the total amount of teredinibactins produced. However, under optimized conditions, ions were observed corresponding to simultaneous incorporation of labeled Cys and Gly, and not a mixture, indicating intact incorporation of the dipeptide (Figure 2, bottom panel).

Cys-Gly was readily incorporated intact into **1** and **2** in both ^{15}N and ^{13}C experiments, with essentially complete incorporation, while Cys itself was also efficiently incorporated into **1** and **2**. Surprisingly, when Cys was added to the medium, an additional new peak was also observed that corresponded to an adduct **1a** that lacked Gly (Figure S1). We have never previously observed this adduct in *T. turnerae* T7901 despite significant experimentation with this strain over a period of years.

These results suggest two possible routes to teredinibactins, both involving sulfur nucleophile addition to an electrophile (Figure 3). In the first, glutathione is added via the action of a glutathione *S*-transferase (GST) enzyme, as proposed for the plant natural product, camalexin.[13] GSTs are also involved in biosynthesis of other sulfur-containing natural products.[18] If so, several possible metabolic fates of a glutathionylated electrophile would be possible. GST adducts, including in natural products, are often hydrolyzed by gamma-glutamyl transpeptidase (GGT) prior to secretion.[19] In the case of teredinibactins, such a hydrolyzed intermediate would be primed to undergo spontaneous thiazoline formation, leading to a stable final product **1** or **2**. Alternatively, if the intermediate is not hydrolyzed quickly enough, the unstable intermediate might be transthiolated to produce compounds such as **1a**. The second possibility is that all of the products observed are generated through non-enzymatic conjugation of Cys-derived nucleophiles with an electrophile. Recent years have seen an increasing number of natural products ascribed to non-enzymatic processes.[20]

In the plants, the electrophilic species that react with Cys-Gly or glutathione contain nitriles.[12, 13] Similarly, the nitrile pharmaceutical vidagliptin is non-enzymatically coupled with Cys and Cys-Gly during mammalian metabolism.[14] Inspired by these precedents, we aimed to couple electrophilic nitriles with Cys-Gly synthetically. 2,4-Dihydroxybenzonitrile was readily prepared, and its halogenated 3-chloro and 3,5-dichloro products were obtained using hypochlorite and purified.[21] Coupling/thiazoline forming reactions used two equivalents of Cys-Gly in methanolic KOH.

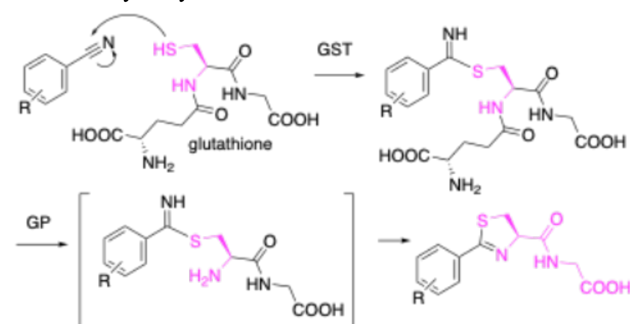

Figure 3. Potential biosynthetic pathway to teredinibactins. Glutathione first reacts as an electrophile, here shown as a nitrile based upon precedents although others are possible, catalyzed by glutathione *S*-transferase (GST). Subsequently, glutathione protease (GP) cleavage and heterocyclization would yield the natural product, or possibly a precursor of the natural product requiring further oxidation. Alternatively, sulfur nucleophiles such as Cys-Gly might add non-enzymatically to an electrophile.

Under this condition, using 2,4-dihydroxbenzonitrile (**3**), natural product **2** was efficiently synthesized (63% yield) at 60 ºC for 24 h. The reaction with 3-chloro-2,4-dihydroxybenzonitrile (**4**) was slower, necessitating an increase to 70 ºC over 72 h and forming **1** in only 12% yield. Comparison of NMR and electronic circular dichroism spectra of purified synthetic **1** and **2** to those of the isolated natural products confirmed their structures and the initial assignment of the C-9 *R* configuration.

To determine whether **1** and **2** might form non-enzymatically under fermentation conditions, the proposed intermediates were added to SBM with sucrose, absent *T. turnerae*. Cys-Gly (2 mM) and an aromatic nitrile (either **3** or **4**, 1 mM) were incubated in the media at the normal bacterial growth temperature, but without bacteria, (30 ºC) for three days. In this condition, **2** was easily identified, but **1** was only present in a small amount (Figure S5). The rate of teredinibactin production was further investigated by NMR. Substrates **3** or **4** (~60 mM) were incubated with Cys-Gly (~120 mM) in phosphate buffer (100 mM, pH 6.4) in an NMR tube, with the probe set at 30 ºC. ^{1}H NMR spectra were acquired every 5 min over 24 h, and the area under the curve (AUC) for the azoline alpha-proton was measured in comparison with a nitrile proton (Figure 4). Compounds **1** and **2** were produced at linear rates over the 24 h period, with yields of 10.7% and 16.7%, respectively.

Overall, both experimental methods reveal that **1** and **2** can be produced non-enzymatically under relevant conditions. Alternatively, the sluggish nature of the reaction suggests that

https://doi.org/10.26434/chemrxiv-2024-ph6m0 **ORCID:** https://orcid.org/0000-0003-3204-3235 Content not peer-reviewed by ChemRxiv. **License:** CC BY-NC-ND 4.0

either the right electrophile has not yet been identified or that the reaction may rely on enzymatic assistance in *T. turnerae*.

Because of the different rate of synthesis of **1** and **2**, we sought to explore the impact of halogens on azoline formation from ß-resorcyclic nitrile. Recently, thiazoline synthesis has seen a Renaissance, with new methods used to produce thiazolines themselves or thiazolines that are convenient intermediates to other compounds. Another application has been the development of protein labeling reactions that exploit in situ azoline formation.[1, 4] In these applications, the rate of thiazoline formation is a key variable that is optimized. Thus, we believed that this synthesis might find applications beyond teredinibactins.

Aromatic nitriles with various halogens were prepared and used in coupling reactions with Cys-Gly (Scheme S1 and Table 1). Under the reaction conditions, in addition to **1** and **2** described above, we synthesized additional teredinibactin analogs **5**, **7**, and **10**, containing 3-Cl, 3,5-Cl_2, 5-Br, and 5-I (Figures S6-16). These previously unreported compounds were obtained in yields of ~16-40%. However, reactions with some of the intermediates failed. Compounds **6** and **9**, with Br or I in the 3-position, respectively, were not successfully synthesized, and starting materials were still present. In all cases, the starting nitrile could still be observed, indicating that differences in product yield after 72 h reflected the relative rates of coupling and not loss of starting material. An exception was that, in the case of the 3,5-dibromo substrate, 3-Br was lost, yielding compound **6** instead of the expected dibromo product **8**. The unreacted substrate itself also lost 3-Br. Di- and tribromoresorcinols have long been known to lose bromine under basic conditions due to their pseudo-quinoid character.[22] Usually, the reactive bromine is para to phenol, however. Overall, it appears that larger halogens in the 3-position of benzonitriles prevent the coupling reaction, and halogens in general greatly decrease the base-catalyzed coupling rate.

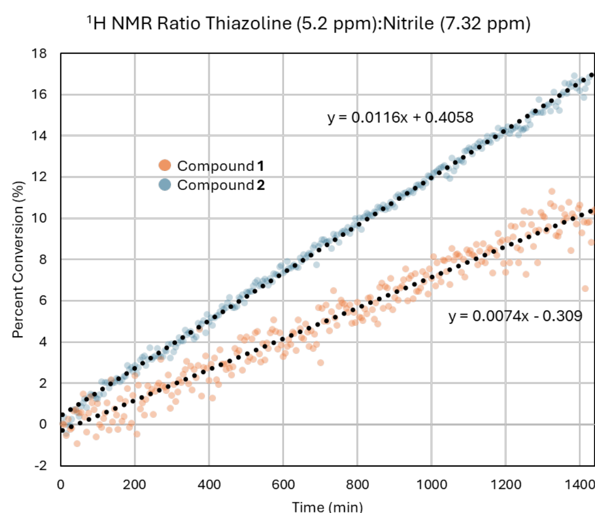

Figure 4. Rate of teredinibactin formation by ^{1}H NMR. Product amounts are given in mM in comparison to the nitrile substrate, which was present at an initial concentration of 70 mM, Cys-Gly initial concentration at 140 mM.

In bacteria, aryl-azolines are usually derived from NRPS biochemistry,[5, 7] but here we show that the metal-binding terdinibactins are instead derived from glutathione. Precedent for direct glutathione or Cys-Gly reaction with nitriles can be found in the indolokines and camalexin from plants, but the reactions have not been characterized in bacteria, to the best of our knowledge. Moreover, the aromatic groups are all derived from indoles, rather than the resorcyclic acid found in teredinibactins. In the case of camalexin, glutathione is cleaved after reaction with the indole substrate, leading to subsequent azoline formation. In another case, firefly luciferin was proposed to evolve from an initial detoxification mechanism,[23] implying that even when detoxification using GST is initially important, the resulting pharmacophores might eventually become fixed in dedicated natural product biosynthetic pathways. Here, based upon these precedents and upon the feeding and model synthetic reactions performed in this study, we propose a noncanonical biosynthetic pathway to teredinibactins. Further, our synthetic study provides reactivity information enabling further development of azoline syntheses for diverse applications.

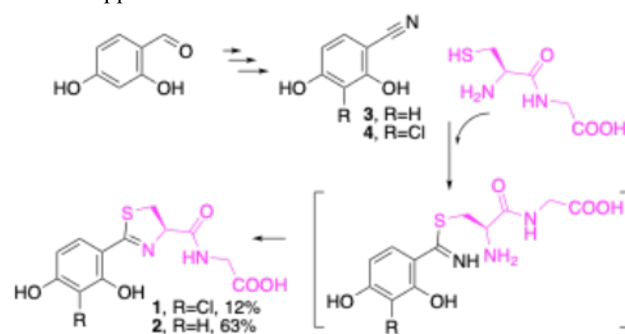

Scheme 1. Synthesis of natural products 1 and 2 using biomimetic conditions.

Table 1. Outcome of coupling reactions with nitrile substrates

Compound	Halogen	yield (%)	observation
1	3-Cl	12	
2	none	63	faster reaction
5	3,5-diCl	40	
6	3-Br	0	
7	5-Br	16	
8	3,5-diBr	N/A	3-Br eliminated
9	3-I	0	
10	5-I	18	

ACKNOWLEDGMENT

We thank the Jack Skalicky and the HSC NMR Core for aid with NMR experiments. This work was funded by NIH R35GM148283 and R01AI162943.

REFERENCES

(1) Kumar, S.; Arora, A.; Sapra, S.; Kumar, R.; Singh, B. K.; Singh, S. K. Recent advances in the synthesis and utility of thiazoline and its derivatives. *RSC Adv.* **2024**, *14* (2), 902-953.

(2) Dunbar, K. L.; Scharf, D. H.; Litomska, A.; Hertweck, C. Enzymatic carbon-sulfur bond formation in natural product biosynthesis. *Chem. Rev.* **2017**, *117* (8), 5521-5577.

(3) Goto, Y.; Ito, Y.; Kato, Y.; Tsunoda, S.; Suga, H. One-pot synthesis of azoline-containing peptides in a cell-free translation system integrated with a posttranslational cyclodehydratase. *Chem. Biol.* **2014**, *21* (6), 766-774.

https://doi.org/10.26434/chemrxiv-2024-ph6m0 **ORCID:** https://orcid.org/0000-0003-3204-3235 Content not peer-reviewed by ChemRxiv. **License:** CC BY-NC-ND 4.0

(4) Proj, M.; Strasek, N.; Pajk, S.; Knez, D.; Sosic, I. Tunable heteroaromatic nitriles for selective bioorthogonal click reaction with cysteine. *Bioconjug. Chem.* **2023**, *34* (7), 1271-1281. Zhu, Y.; Zhang, X.; You, Q.; Jiang, Z. Recent applications of CBT-Cys click reaction in biological systems. *Bioorg. Med. Chem.* **2022**, *68*, 116881.

(5) Gehring, A. M.; DeMoll, E.; Fetherston, J. D.; Mori, I.; Mayhew, G. F.; Blattner, F. R.; Walsh, C. T.; Perry, R. D. Iron acquisition in plague: modular logic in enzymatic biogenesis of yersiniabactin by *Yersinia pestis*. *Chem. Biol.* **1998**, *5* (10), 573-586.

(6) Li, Y. M.; Milne, J. C.; Madison, L. L.; Kolter, R.; Walsh, C. T. From peptide precursors to oxazole and thiazole-containing peptide antibiotics: microcin B17 synthase. *Science* **1996**, *274* (5290), 1188-1193.

(7) Gehring, A. M.; Mori, I.; Perry, R. D.; Walsh, C. T. The nonribosomal peptide synthetase HMWP2 forms a thiazoline ring during biogenesis of yersiniabactin, an iron-chelating virulence factor of *Yersinia pestis*. *Biochemistry* **1998**, *37* (33), 11637-11650.

(8) Miller, B. W.; Schmidt, E. W.; Concepcion, G. P.; Haygood, M. G. Halogenated metal-binding compounds from shipworm symbionts. *J. Nat. Prod.* **2022**, *85* (3), 479-484.

(9) Yang, J. C.; Madupu, R.; Durkin, A. S.; Ekborg, N. A.; Pedamallu, C. S.; Hostetler, J. B.; Radune, D.; Toms, B. S.; Henrissat, B.; Coutinho, P. M.; et al. The complete genome of Teredinibacter turnerae T7901: an intracellular endosymbiont of marine wood-boring bivalves (shipworms). *PLoS One* **2009**, *4* (7), e6085. Altamia, M. A.; Lin, Z.; Trindade-Silva, A. E.; Uy, I. D.; Shipway, J. R.; Wilke, D. V.; Concepcion, G. P.; Distel, D. L.; Schmidt, E. W.; Haygood, M. G. Secondary metabolism in the gill microbiota of shipworms (Teredinidae) as revealed by comparison of metagenomes and nearly complete symbiont genomes. *mSystems* **2020**, *5* (3).

(10) Miller, B. W.; Lim, A. L.; Lin, Z.; Bailey, J.; Aoyagi, K. L.; Fisher, M. A.; Barrows, L. R.; Manoil, C.; Schmidt, E. W.; Haygood, M. G. Shipworm symbiosis ecology-guided discovery of an antibiotic that kills colistin-resistant *Acinetobacter*. *Cell Chem. Biol.* **2021**, *28* (11), 1628-1637 e1624. Altamia, M. A.; Distel, D. L. Transport of symbiont-encoded cellulases from the gill to the gut of shipworms via the enigmatic ducts of Deshayes: a 174-year mystery solved. *Proc. Biol. Sci.* **2022**, *289* (1986), 20221478.

(11) Kim, C. S.; Li, J. H.; Barco, B.; Park, H. B.; Gatsios, A.; Damania, A.; Wang, R.; Wyche, T. P.; Piizzi, G.; Clay, N. K.; et al. Cellular atress upregulates indole signaling metabolites in *Escherichia coli*. *Cell Chem. Biol.* **2020**, *27* (6), 698-707 e697.

(12) Rajniak, J.; Barco, B.; Clay, N. K.; Sattely, E. S. A new cyanogenic metabolite in *Arabidopsis* required for inducible pathogen defence. *Nature* **2015**, *525* (7569), 376-379. Klein, A. P.; Anarat-Cappillino, G.; Sattely, E. S. Minimum set of cytochromes P450 for reconstituting the biosynthesis of camalexin, a major *Arabidopsis* antibiotic. *Angew. Chem. Int. Ed. Engl.* **2013**, *52* (51), 13625-13628.

(13) Mucha, S.; Heinzlmeir, S.; Kriechbaumer, V.; Strickland, B.; Kirchhelle, C.; Choudhary, M.; Kowalski, N.; Eichmann, R.; Huckelhoven, R.; Grill, E.; et al. The formation of a camalexin biosynthetic metabolon. *Plant Cell* **2019**, *31* (11), 2697-2710.

(14) Mizuno, K.; Takeuchi, K.; Umehara, K.; Nakajima, M. Identification of a novel metabolite of vildagliptin in humans: Cysteine targets the nitrile moiety to form a thiazoline ring. *Biochem. Pharmacol.* **2018**, *156*, 312-321. Mizuno, K.; Takeuchi, K.; Umehara, K.; Nakajima, M. Identification of novel metabolites of vildagliptin in rats: thiazoline-containing thiol adducts formed via cysteine or glutathione conjugation. *Drug Metab. Dispos.* **2019**, *47* (8), 809-817.

(15) Fahey, R. C. Glutathione analogs in prokaryotes. *Biochim. Biophys. Acta* **2013**, *1830* (5), 3182-3198.

(16) Waterbury, J. B.; Calloway, C. B.; Turner, R. D. A cellulolytic nitrogen-fixing bacterium cultured from the gland of Deshayes in shipworms (Bivalvia: Teredinidae). *Science* **1983**, *221* (4618), 1401-1403.

(17) Liebergesell, T. C. E.; Puri, A. W. Linking biosynthetic genes to natural products using inverse stable isotopic labeling (InverSIL). *Methods Enzymol.* **2024**, *702*, 215-227. Liebergesell, T. C. E.; Murdock, E. G.; Puri, A. W. Detection of inverse stable isotopic labeling in untargeted metabolomic data. *Anal. Chem.* **2024**, *96* (41),16330-16337.

(18) Scharf, D. H.; Remme, N.; Habel, A.; Chankhamjon, P.; Scherlach, K.; Heinekamp, T.; Hortschansky, P.; Brakhage, A. A.; Hertweck, C. A dedicated glutathione *S*-transferase mediates carbon-sulfur bond formation in gliotoxin biosynthesis. *J. Am. Chem. Soc.* **2011**, *133* (32), 12322-12325.

(19) Ito, T.; Kitaiwa, T.; Nishizono, K.; Umahashi, M.; Miyaji, S.; Agake, S. I.; Kuwahara, K.; Yokoyama, T.; Fushinobu, S.; Maruyama-Nakashita, A.; et al. Glutathione degradation activity of gamma-glutamyl peptidase 1 manifests its dual roles in primary and secondary sulfur metabolism in *Arabidopsis*. *Plant J.* **2022**, *111* (6), 1626-1642.

(20) Aniebok, V.; Shingare, R. D.; Wei-Lee, H.; Johnstone, T. C.; MacMillan, J. B. Biomimetic total synthesis and investigation of the non-enzymatic chemistry of oxazinin A. *Angew. Chem. Int. Ed. Engl.* **2022**, *61* (38), e202208029.

(21) Noel, S.; Hoegy, F.; Rivault, F.; Rognan, D.; Schalk, I. J.; Mislin, G. L. Synthesis and biological properties of thiazole-analogues of pyochelin, a siderophore of *Pseudomonas aeruginosa*. *Bioorg. Med. Chem. Lett.* **2014**, *24* (1), 132-135. Serrano, J. L.; Sierra, T.; Gonzalez, Y.; Bolm, C.; Magnus, A.; Moll, G.; Bolm, C.; Weickhardt, K. Improving FLC properties. Simplicity, planarity, and rigidity in new chiral oxazoline derivatives. *J. Am. Chem. Soc.* **1995**, *117* (32), 8312-8321. Tan, J. S.; Ciufolini, M. A. Total synthesis of topopyrones B and D. *Org. Lett.* **2006**, *8* (21), 4771-4774.

(22) Davis, T. L.; Harrington, V. F. The pseudo-quinoid character of tribromoresorcinol. *J. Am. Chem. Soc.* **1934**, *56* (1), 129-132.

(23) de Souza, D. R.; Silva, J. R.; Moreira, A.; Viviani, V. R. Biosensing firefly luciferin synthesis in bacteria reveals a cysteine-dependent quinone detoxification route in *Coleoptera*. *Sci. Rep.* **2022**, *12* (1), 14815.

https://doi.org/10.26434/chemrxiv-2024-ph6m0 **ORCID:** https://orcid.org/0000-0003-3204-3235 Content not peer-reviewed by ChemRxiv. **License:** CC BY-NC-ND 4.0

Supporting Information for:

Glutathione in the noncanonical biosynthesis of teredinibactins

Youjung Sung, Bailey W. Miller, and Eric W. Schmidt

Methods

General experimental methods. LC-MS was run on a Waters Xevo G2-XS-QTOF LC-MS in positive mode with a C18 column. HPLC was run on Thermo UltiMate 3000 system which had the solvent system H_2O (0.01% TFA) and acetonitrile. High performance flash chromatography was performed on high performance GOLD 15.5 g HP C18 column with the solvent system H_2O (0.01% TFA) and acetonitrile. NMR data were collected on a Varian 500 MHz spectrometer using CD_3OD, DMSO-d6, or D_2O as solvents. ECD experiments were conducted on Aviv Biomedical, Inc. Circular Dichroism Spectrometer Model 410 using compounds at 1 mg /ml in methanol. Spectra were collected in wavelength 180 – 450 nm (bandwidth 1 nm, 25 °C). The ECD spectra used here were average values of triplicate measurements.

Teredinibacter turnerae T7901 culture conditions. Shipworm Basal Media (SBM) is based upon a recipe from Waterbury, et al. 1983, with modifications. The complete recipe is as follows: SBM (1 L) is prepared by autoclaving Instant Ocean (750 mL, 36 g/L), ddH_2O (197 mL), and 10% ammonium chloride (2.5 mL). To this medium are added 1 M HEPES buffer (pH=8.0, 20 mL), metal and minerals master mix (15 mL), and a carbon source (10% solution in dd H_2O, 20 mL). In this work, the carbon source used was glucose. In solid media, 1% agar was added.

The metal and minerals master mix includes the following in a final volume of 150 mL: Na_2CO_3 (40 mM), Na_2MoO_4 (10 mM), EDTA (0.5 mM), ferric ammonium citrate (4.5 mM), citric acid (5.7 mM), K_2HPO_4 (45 mM), and A-5 metal mix (10 mL). A-5 metal mix is comprised of (per liter): H_3BO_3 (2.86 g), $MnCl_2$-4H_2O (1.81 g), Na_2MoO_4-2H_2O (0.039 g), $CuSO_4$-5H_2O (0.079 g), $Co(NO_3)2$-6H_2O (0.494 g).

T. turnerae was revived from glycerol stocks on (SBM) plates with 0.2% glucose. Individual colonies were picked from plates and used to inoculate seed cultures in liquid SMB, which were then used to inoculate experimental cultures at 30°C with shaking at 200 rpm.

Mass spectrometric method for detection of teredinibactin derivatives in extracts. Waters Xevo G2-XS-QTOF LC-MS was used with the solvent system: A (Optima LC-MS grade water with 0.1 % formic acid) and B (Optima LC-MS grade acetonitrile with 0.1 % formic acid). Waters Acquity UPLC HSS T3 1.8 um T3 column (2.1 x 100 mm) was run with linear gradient: 0 – 0.5 min, 1% B in A; 0.5 – 7.5 min, 1 – 100% B in A; 7.5 – 9 min, 100% B in A; 9 – 9.5 min, 100 – 1 % B in A; 9.5 – 10 min 1% B in A, flow rate: 0.3 ml/min. Waters Acquity UPLC BEH C18 1.7 um C18 column (2.1 x 50 mm) was run on the method with linear gradient: 0 – 0.1 min, 5% B in A; 0.1 – 7 min, 5 – 100% B in A; 7 – 8 min, 100% B in A; 8 – 8.5 min, 100 – 5 % B in A; 8.5 – 9 min 5% B in A, flow rate: 0.6 ml/min. The NMR data was collected on Varian 500 MHz NMR spectrometer.

Stable isotope labeling studies. SBM medium was made as described above, except that either U-^{13}C-D-glucose or $^{15}NH_4Cl$ were used to replace the natural abundance ingredients. *T. turnerae* T7901 was cultured for 1 d in 5 mL of SBM with 0.2% glucose at 30°C, 200 rpm, and then a nucleophile (Cys, Cys-Gly, or reduced glutathione, each at 5 mM dissolved in water) was added to the culture. On day 6, the bacterial culture was harvested by centrifugation (4000 x *g*, 15 min). The supernatant was decanted and extracted with ethyl acetate. Teredinibactins were observed in the aqueous partition, which was diluted 1:5 in 50% aqueous methanol for analysis by UPLC-MS as described above, in comparison with the previously described unlabeled teredinibactins **1** and **2**.[8] Each analysis was completed at least in duplicate.

Synthesis of 2,4-dihydroxybenzonitrile (**3**). Following the approach of Serrano et al.,[21] 2,4-Dihydroxybenzaldehyde (**11**) (5.5 g, 40 mmol) was dissolved in ethanol (15 ml), and $NH_2OH{\cdot}HCl$ (4.2 g, 60 mmol) was slowly added. To this solution, Na_2CO_3 (6.4 g, 60 mmol) in water (15 ml) was added, and the mixture was stirred for 6 h at 20 °C. The reaction mixture was washed with ice cold water and dried under vacuum. The 2,4-dihydroxybenzaldehyde oxime (**12**) (3.0 g, 19.6 mmol) was mixed with Ac_2O (18 ml) and refluxed for 3 h at 125 °C. The mixture was cooled to room temperature and dried under vacuum. The dried product was dissolved in ethyl acetate and washed with supersaturated $NaHCO_3$ in water. The organic phase was dried under vacuum. KOH (3.5 g) in methanol (15 ml) was added to the crude product, and the solution was stirred for 1 d at room temperature. The reaction mixture was acidified with sulfuric acid to pH 2.0 and extracted with ethyl acetate. The organic phase was dried under vacuum. 2,4-Dihydroxybenzonitrile (**3**) was isolated as a brown amorphous solid (1.9 g, 13.7 mmol, 70% yield) with m/z = 134.0251 [M-H]$^-$; calcd for $C_7H_4NO_2^-$ m/z = 134.0248. ^{1}H NMR (500

https://doi.org/10.26434/chemrxiv-2024-ph6m0 ORCID: https://orcid.org/0000-0003-3204-3235 Content not peer-reviewed by ChemRxiv. License: CC BY-NC-ND 4.0

MHz, CD_3OD) δ 7.20 (d, *J* = 8.5 Hz, 1H), 6.33 (s, 1H), 6.31 (d, *J* = 8.4 Hz, 1H); ^{13}C NMR (126 MHz, CD_3OD) δ 162.8, 161.8, 134.6, 117.7, 108.3, 102.4, 89.8.

Synthesis of 3-chloro-2,4-dihydroxybenzonitrile (**4**) and 3,5-dichloro-2,4-dihydroxybenzonitrile (**13**). The general method followed the work of Tan et al, but we used **3** as our substrate.[21] To **3** (135.1 mg, 1 mmol) in water (0.69 ml), was added KOH (137.9 mg, 2.5 mmol) in water (1.03 ml). Subsequently, commercial bleach (1.8 ml, 1.4 mmol) was added at room temperature. The reaction mixture was stirred for 3 h, acidified with 6M HCl (1.38 ml), and extracted with EtOAc (3 x 3 ml). The organic layer was dried with Na_2SO_4 and concentrated with a rotary evaporator. Separation used CombiFlash purification with a high-performance GOLD 15.5 g HP C18 and solvent system: 0.01 % TFA in water (A) and HPLC grade acetonitrile (B), gradient 20 – 55 % acetonitrile in water for 12 min, followed by 100 % acetonitrile at 40 ml/min. After drying, 3-chloro-2,4-dihydroxybenzonitrile (**4**) (95.0 mg, 0.6 mmol, 56% yield) and 3,5-dichloro-2,4-dihydroxybenzonitrile (**13**) (23.2 mg, 0.1 mmol, 11% yield) were obtained.

3-Chloro-2,4-dihydroxybenzonitrile (**4**) was isolated as a white amorphous solid with *m/z* = 167.9869 $[M-H]^-$; calcd for $C_7H_3ClNO_2^-$, *m/z* = 167.9858. ^{1}H NMR (500 MHz, CD_3OD) δ 7.27 (d, *J* = 8.7 Hz, 1H), 6.51 (d, *J* = 8.6 Hz, 1H).

3,5-Dichloro-2,4-dihydroxybenzonitrile (**13**) was isolated as a white amorphous solid with *m/z* = 201.9468 $[M-H]^-$; calcd for $C_7H_2Cl_2NO_2^-$, *m/z* = 201.9468. ^{1}H NMR (500 MHz, CD_3OD) δ 7.41 (s, 1H).

Synthesis of teredinibactin A (**1**). Following the approach of Noël et al.,[21] compound **4** (20 mg, 0.118 mmol) was dissolved in degassed MeOH (0.75 ml), and mixed with L-cysteinylglycine (42.0 mg, 0.24 mmol, 2 equiv.) in pH 6.4 phosphate buffer (0.5 ml) and stirred at 70°C for 72h. HPLC method was 20 % acetonitrile in water (0.01 % TFA) at flow rate 3.5 ml/min for 20 min with a Luna 5u C18 (250 x 10 mm) column. Teredinibactin A (**1**) was isolated as a brown amorphous solid (4.7 mg, 0.014 mmol, 12% yield) with *m/z* = 331.0149 $[M+H]^+$; calcd for $C_{12}H_{12}ClN_2O_5S^+$, *m/z* = 331.0150. ^{1}H NMR (500 MHz, CD_3OD) δ 7.33 (d, *J* = 8.6 Hz, 1H), 6.52 (d, *J* = 8.7 Hz, 1H), 5.34 (t, *J* = 8.8 Hz, 1H), 4.00 (d, *J* = 10.0 Hz, 1H), 3.74 (dd, *J* = 11.5, 7.95 Hz, 1H), 3.64 (dd, *J* = 11.1, 7.8 Hz, 1H) and ^{13}C NMR (126 MHz, CD_3OD) δ 174.4, 171.8, 171.3, 158.0, 156.7, 129.3, 109.3, 107.7, 107.0, 77.4, 40.6, 33.3.

Synthesis of dechloroteredinibactin (**2**). Following the approach of Noël et al.[21], 2,4-dihydroxybenzonitrile (**3**) (68.6 mg, 0.5 mmol) was dissolved in degassed MeOH (2.2 ml), mixed with L-cysteinylglycine (178.2 mg, 1 mmol, 2 equiv.) in pH 6.4 phosphate buffer (2.2 ml), and stirred at 60 °C for 24 h. HPLC method was 15 % acetonitrile in water (0.01 % TFA) at flow rate 3.5 ml/min for 30 min with a Luna 5u C18 (250 x 10 mm) column. Dechloroteredinibactin (**2)** was isolated as an orange amorphous solid (42.56 mg, 0.32 mmol, 63% yield) with *m/z* = 297.0538 $[M+H]^+$; calcd for $C_{12}H_{13}N_2O_5S^+$, *m/z* = 297.0540. ^{1}H NMR (500 MHz, DMSO-d_6) δ 12.19 (brs, 1H), 10.42 (brs, 1H), 8.46 (t, *J* = 5.9 Hz, 1H), 7.28 (d, *J* = 8.6 Hz, 1H), 6.38 (dd, *J* = 8.6, 2.4 Hz, 1H), 6.31 (d, *J* = 2.3 Hz, 1H), 5.29 (dd, *J* = 9.4, 8.2 Hz, 1H), 3.79 (d, *J*= 5.8 Hz, 2H), 3.62 (dd, *J* = 11.0, 9.4 Hz, 1H), 3.48 (dd, *J* = 11.0, 8.2 Hz, 1H) and ^{13}C NMR (126 MHz, DMSO-d_6) δ 172.5, 171.4, 170.4, 162.7, 160.7, 132.7, 108.8, 108.4, 102.7, 77.7, 41.4, 33.6.

Testing the non-enzymatic coupling hypothesis. Sterile SBM medium (1% sucrose) was prepared. To 5 mL SBM sucrose culture aliquots were added sterile reagents L-cysteinylglycine (2 mM) and a nitrile (1 mM), either 2,4-dihydroxy benzonitrile (**3**) or 3-chloro-2,4-dihydroxy benzonitrile (**4**), and the reactions were run for 72 h at 30 °C , mimicking culture conditions but without bacteria. Additional experiments were performed to which were added aromatic compounds (1 mM) 2,4-dihydroxy benzoic acid, 2,4-dihydroxy benzaldehyde, 3-chloro-2,4-dihydroxy benzoic acid, or 3-chloro-2,4-dihydroxy benzaldehyde instead of nitriles. The mixtures were extracted with ethyl acetate three times, dried under vacuum, resuspended in methanol, and analyzed by UPLC-MS as described above.

The non-enzymatic reaction rate was monitored by NMR. A solution was prepared in a 5 mm NMR tube consisting of phosphate buffer (pH 6.4, 0.1 M in D_2O, 324 μl) and L-cysteinylglycine (0.05 mmol). To this solution was added either nitrile **3** or **4** (0.025 mmol) dissolved in CD_3OD (36 μl). The mixtures were maintained at 30 °C in the probe, and progress of each reaction was monitored by measuring the ^{1}H spectrum every 5 min over a 24-h period. The signals for the a-proton of thiazoline and the aromatic nitrile were integrated and compared to determine yield of reaction at each time point. Integral areas were normalized to a starting azoline concentration of 0.

Synthesis of 3-bromo-2,4-dihydroxybenzonitrile (**14**), 5-Bromo-2,4-dihydroxybenzonitrile (**15**) and 3,5-dibromo-2,4-dihydroxybenzonitrile (**16**). We followed the general method in Tan et al. but using substrate **3**.[21] To 2,4-dihydroxybenzonitrile (**3**) (62.5 mg, 0.5 mmol) in methanol (2.5 ml) was added NBS (89.0 mg, 0.5 mmol) at 0

https://doi.org/10.26434/chemrxiv-2024-ph6m0 **ORCID:** https://orcid.org/0000-0003-3204-3235 Content not peer-reviewed by ChemRxiv. **License:** CC BY-NC-ND 4.0

°C. The reaction was stirred for 1 h. Na_2SO_3 (126.1 mg, 1 mmol) and NaOH (40 mg, 1 mmol) in water (2.5 ml) were added to the mixture and stirred for an additional hour. pH was then adjusted to 1.0 with concentrated HCl, and the mixture extracted with EtOAc (5 x 3 ml). The organic layer was dehydrated with Na_2SO_4 and dried with a rotary evaporator. The extract was purified by HPLC on a phenylhexyl column (250 x 10 mm) with 35 % acetonitrile in water (0.01 % TFA) at 4 ml/min. 3-Bromo-2,4-dihydroxy benzonitrile (**14**) (27.0 mg, 0.13 mmol, 26% yield), 5-bromo-2,4-dihydroxybenzonitrile (**15**) (3.6 mg, 0.02 mmol, 4% yield), and 3,5-dibromo-2,4-dihydroxy benzonitrile (**16**) (3.5 mg, 0.01 mmol, 2% yield) were isolated.

3-Bromo-2,4-dihydroxybenzonitrile (**14**) was isolated as white amorphous solid with *m/z* = 211.9356 $[M-H]^-$; calcd for $C_7H_3BrNO_2^-$, *m/z* = 211.9353. ^{1}H NMR (500 MHz, a CD_3OD) δ 7.34 (d, *J* = 8.6 Hz, 1H), 6.51 (d, *J* = 8.6 Hz, 1H).

5-Bromo-2,4-dihydroxybenzonitrile (**15**) was isolated as a white amorphous solid with *m/z* = 211.9356 $[M-H]^-$; calcd for $C_7H_3BrNO_2^-$, *m/z* = 211.9353. ^{1}H NMR (500 MHz, CD_3OD) δ 7.58 (s, 1H), 6.52 (s, 1H).

3,5-Dibromo-2,4-dihydroxybenzonitrile (**16**) was isolated as a white amorphous solid with *m/z* = 289.8422 $[M-H]^-$; calcd for $C_7H_2Br_2NO_2^-$, *m/z* = 289.8458. ^{1}H NMR (500 MHz, CD_3OD) δ 7.70 (s, 1H).

Synthesis of 3-iodo-2,4-dihydroxybenzonitrile (**17**) and 5-iodo-2,4-dihydroxybenzonitrile (**18**). We followed the approach of Tan et al. but using different substrates.[21] We added iodine (111.67 mg, 0.44 mmol) and potassium iodate (42.8 mg, 0.2 mmol) to 2,4-dihydroxybenzonitrile (**3**) (135.12 mg, 1 mmol) in water (1.2 ml) and ethanol (0.76 ml) at room temperature. The reaction was stirred overnight and then diluted with water. After extracting with EtOAc three times, the organic layer was dried with Na_2SO_4 and concentrated with rotary evaporator. The extract was run on HPLC for purification. The HPLC system was 20 % acetonitrile in water (0.01 % TFA) at flow rate 4 ml/min. 3-iodo-2,4-dihydroxy benzonitrile (**17**) (10 mg, 0.04 mmol, 9% yield) and 5-iodo-2,4-dihydroxy benzonitrile (**18**) (99.41 mg, 0.38 mmol, 86% yield) were purified.

3-Iodo-2,4-dihydroxybenzonitrile (**17**) was isolated as a white amorphous solid with *m/z* = 259.9216 $[M-H]^-$; calcd for $C_7H_3INO_2^-$, *m/z* = 259.9214. ^{1}H NMR (500 MHz, CD_3OD) δ 7.35 (d, *J* = 8.5 Hz, 1H), 6.48 (d, *J* = 8.6 Hz, 1H).

5-Iodo-2,4-dihydroxybenzonitrile (**18**) was isolated as a white amorphous solid with *m/z* = 259.9216 $[M-H]^-$; calcd for $C_7H_3INO_2^-$, *m/z* = 259.9214. ^{1}H NMR (500 MHz, CD_3OD) δ 7.69 (s, 1H), 6.44 (s, 1H).

2.4.2.7 Teredinibactin analog (**5**)

13 (20 mg, 0.098 mmol) was dissolved in degassed MeOH (0.55 ml), and mixed with L-cysteinylglycine (35.0 mg, 0.196 mmol, 2 equiv.) in pH 6.4 phosphate buffer (0.35 ml) and stirred at 70°C for 72h. HPLC method was 30 % acetonitrile in water (0.01 % TFA) at flow rate 3.5 ml/min for 27 min with a Luna 5u C18 (250 x 10 mm) column. Compound **5** was isolated as a brown amorphous solid (14.49 mg, 0.04 mmol, 40% yield) with *m/z* = 364.9769 $[M+H]^+$; calcd for $C_{12}H_{11}Cl_2N_2O_5S^+$ *m/z* = 364.9760. ^{1}H NMR (500 MHz, CD_3OD) δ 7.39 (s, 1H), 5.36 (t, *J* = 8.9 Hz, 1H), 4.00 (d, *J* = 9.1 Hz, 1H), 3.75 (dd, *J* = 11.2, 9.4 Hz, 1H), 3.67 (dd, *J* = 11.2, 8.3 Hz, 1H) and ^{13}C NMR (126 MHz, CD_3OD) δ 173.4, 171.4, 155.3, 128.5, 111.9, 109.3, 77.5, 40.7, 33.5.

2.4.2.8 Teredinibactin analog (**7**)

15 (15 mg, 0.07 mmol) was dissolved in degassed MeOH (0.39 ml), and mixed with L-cysteinylglycine (25.0 mg, 0.14 mmol, 2 equiv.) in pH 6.4 phosphate buffer (0.25 ml) and stirred at 70°C for 72h. HPLC method was 30 % acetonitrile in water (0.01 % TFA) at flow rate 3.5 ml/min for 27 min with a Luna 5u C18 (250 x 10 mm) column. Compound **7** was isolated as a brown amorphous solid (4.26 mg, 0.011 mmol, 16% yield) with *m/z* = 374.9647 $[M+H]^+$; calcd for $C_{12}H_{12}BrN_2O_5S^+$ *m/z* = 374.9645. ^{1}H NMR (500 MHz, CD_3OD) δ 7.56 (s, 1H), 6.49 (s, 1H), 5.31 (d, *J* = 8.8 Hz, 1H), 3.98 (d, *J* = 10.7 Hz, 2H), 3.74 (t, *J* = 10.2 Hz, 1H), 3.65 (t, *J* = 8.8 Hz, 1H) and ^{13}C NMR (126 MHz, CD_3OD) δ 173.0, 168.3, 161.6, 161.6, 136.3, 132.0, 111.2, 104.5, 101.9, 77.3, 42.4, 35.3.

2.4.2.9 Teredinibactin analog (**10**)

18 (20 mg, 0.077 mmol) was dissolved in degassed MeOH (0.43 ml), and mixed with L-cysteinylglycine (27.3 mg, 0.153 mmol, 2 equiv.) in pH 6.4 phosphate buffer (0.28 ml) and stirred at 70°C for 72h. HPLC method was 30 % acetonitrile in water (0.01 % TFA) at flow rate 3.5 ml/min for 27 min with a Luna 5u C18 (250 x 10 mm) column. Compound **10** was isolated as a brown amorphous solid (5.78 mg, 0.014 mmol, 18% yield) with *m/z* = 422.9508 $[M+H]^+$; calcd for $C_{12}H_{12}IN_2O_5S^+$ *m/z* = 422.9506. ^{1}H NMR (500 MHz, CD_3OD) δ 7.76 (s, 1H), 6.46 (s, 1H), 5.30 (d, *J* = 8.9 Hz, 1H), 3.98 (d, *J* = 11.05 Hz, 2H), 3.70 (t, *J* = 10.5 Hz, 1H), 3.62 (dd, *J* = 17.8, 9.4 Hz, 1H) and ^{13}C NMR (126 MHz, CD_3OD) δ 172.8, 171.8, 161.2, 154.0, 147.9, 140.6, 111.2, 101.7, 77.8, 39.1, 33.3, 29.3.

https://doi.org/10.26434/chemrxiv-2024-ph6m0 **ORCID:** https://orcid.org/0000-0003-3204-3235 Content not peer-reviewed by ChemRxiv. **License:** CC BY-NC-ND 4.0

Scheme S1. Synthesis of teredinibactin analogs.

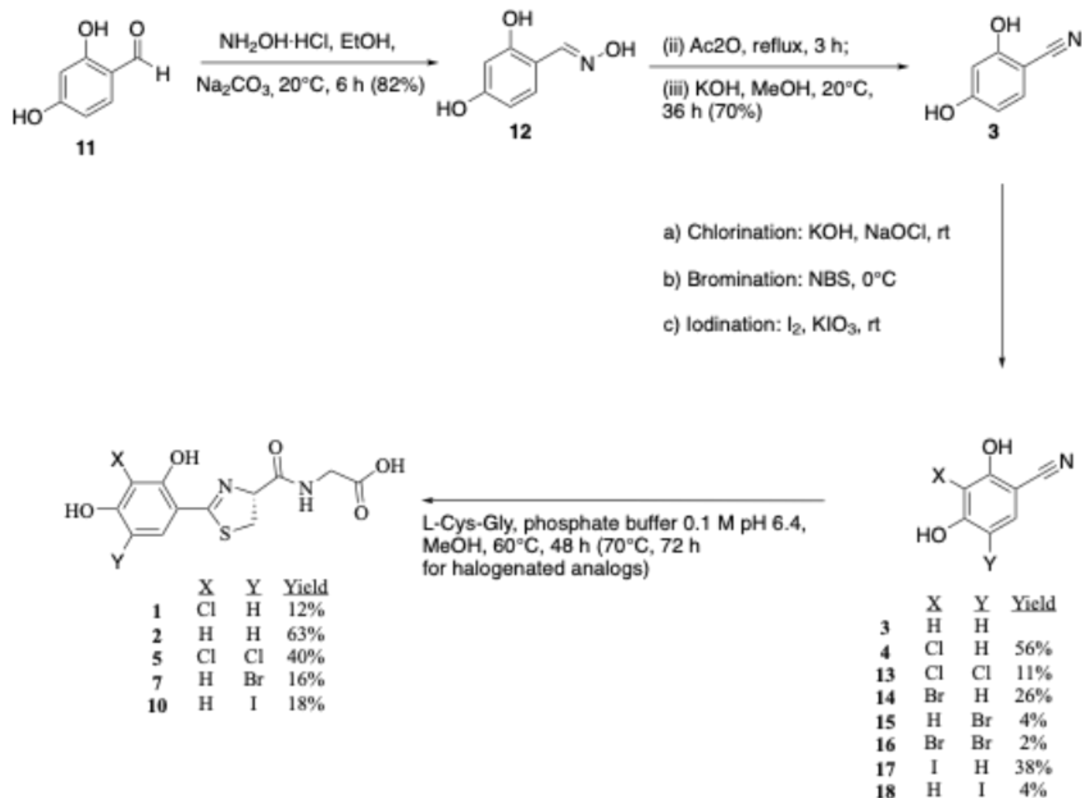

	X	Y	Yield
1	Cl	H	12%
2	H	H	63%
5	Cl	Cl	40%
7	H	Br	16%
10	H	I	18%

	X	Y	Yield
3	H	H	
4	Cl	H	56%
13	Cl	Cl	11%
14	Br	H	26%
15	H	Br	4%
16	Br	Br	2%
17	I	H	38%
18	H	I	4%

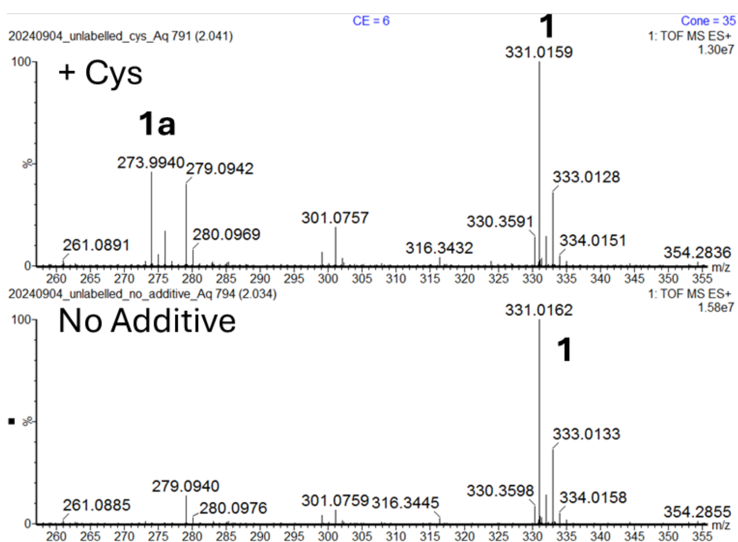

Figure S1. Formation of new compound **1a** (cysteine adduct) with supplementation of cysteine in media.

https://doi.org/10.26434/chemrxiv-2024-ph6m0 **ORCID:** https://orcid.org/0000-0003-3204-3235 Content not peer-reviewed by ChemRxiv. **License:** CC BY-NC-ND 4.0

cl_teredinibactin_1H_CD3OD_04112023
z0gmap_calib

CARBON_01

Figure S2. ^{1}H NMR and ^{13}C NMR spectra of teredinibactin A (**1**).

https://doi.org/10.26434/chemrxiv-2024-ph6m0 **ORCID:** https://orcid.org/0000-0003-3204-3235 Content not peer-reviewed by ChemRxiv. **License:** CC BY-NC-ND 4.0

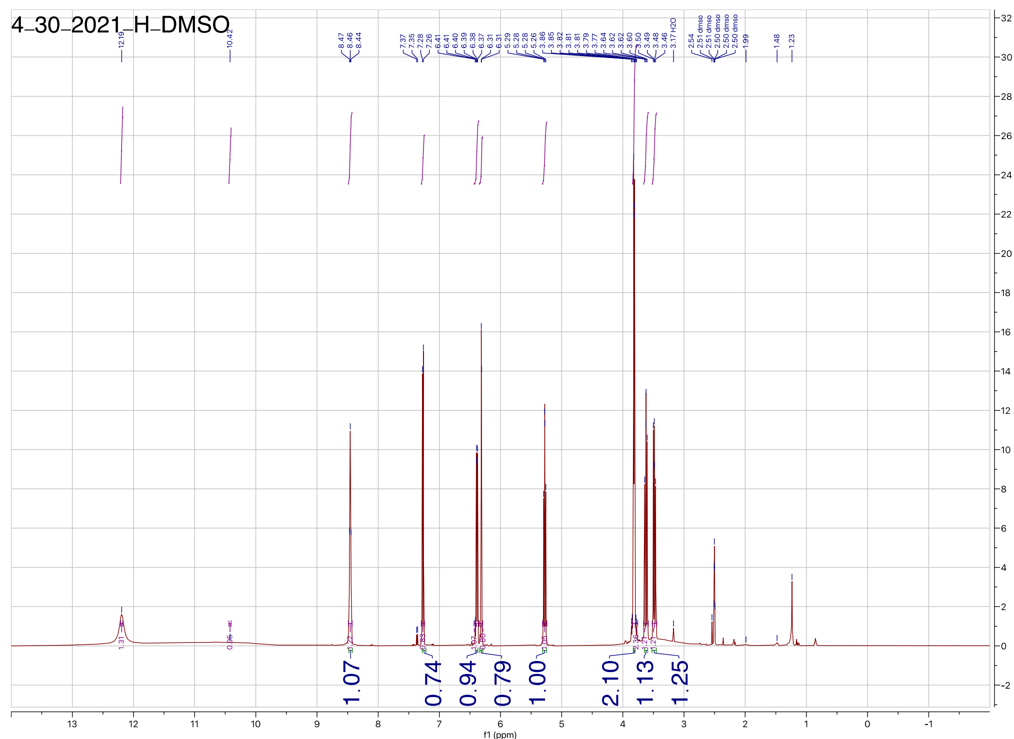

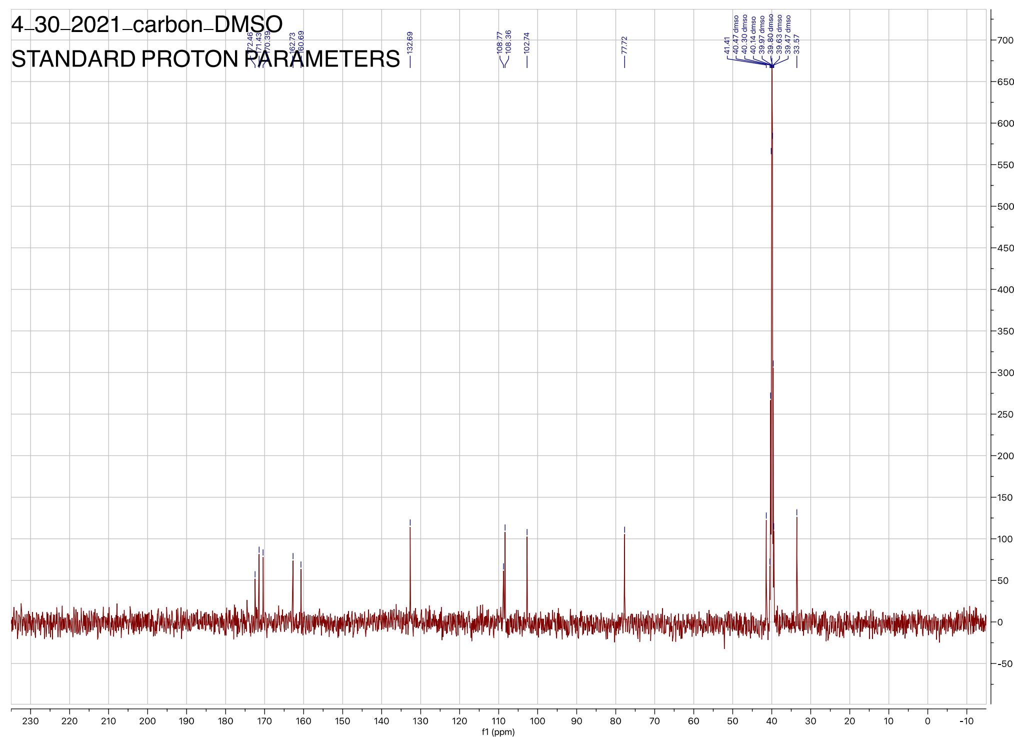

Figure S3. ^{1}H NMR and ^{13}C NMR spectra of dechloroteredinibactin (**2**).

https://doi.org/10.26434/chemrxiv-2024-ph6m0 **ORCID:** https://orcid.org/0000-0003-3204-3235 Content not peer-reviewed by ChemRxiv. **License:** CC BY-NC-ND 4.0

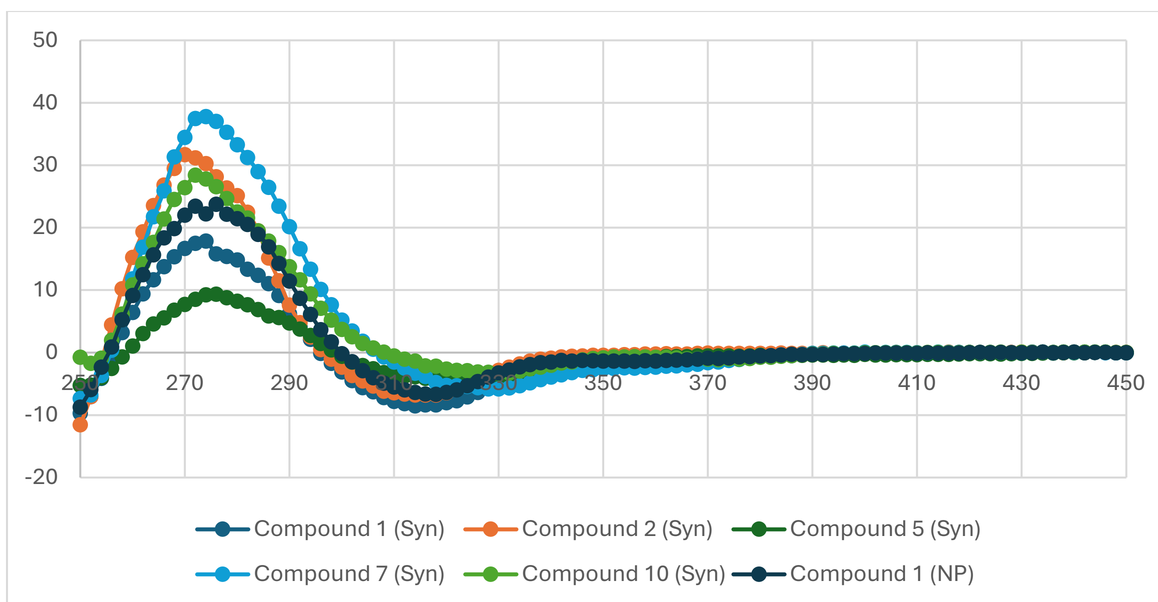

Figure S4. Electronic circular dichroism spectra. Syn: synthetic, NP: natural product.

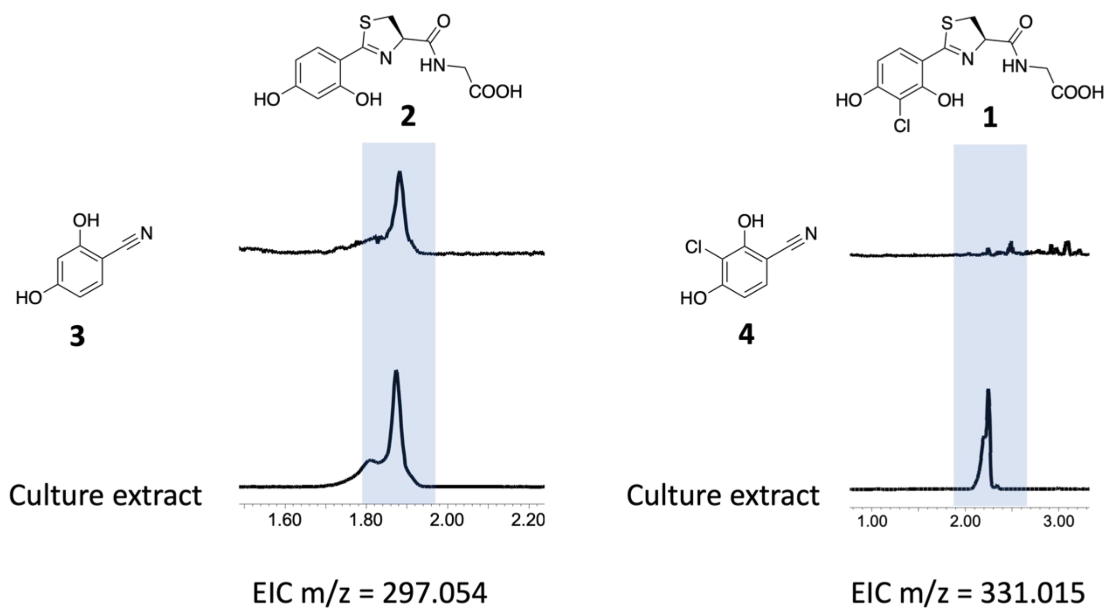

Figure S5. Non-enzymatic coupling of nitriles with Cys-Gly in sterile SBM medium.

https://doi.org/10.26434/chemrxiv-2024-ph6m0 **ORCID:** https://orcid.org/0000-0003-3204-3235 Content not peer-reviewed by ChemRxiv. **License:** CC BY-NC-ND 4.0

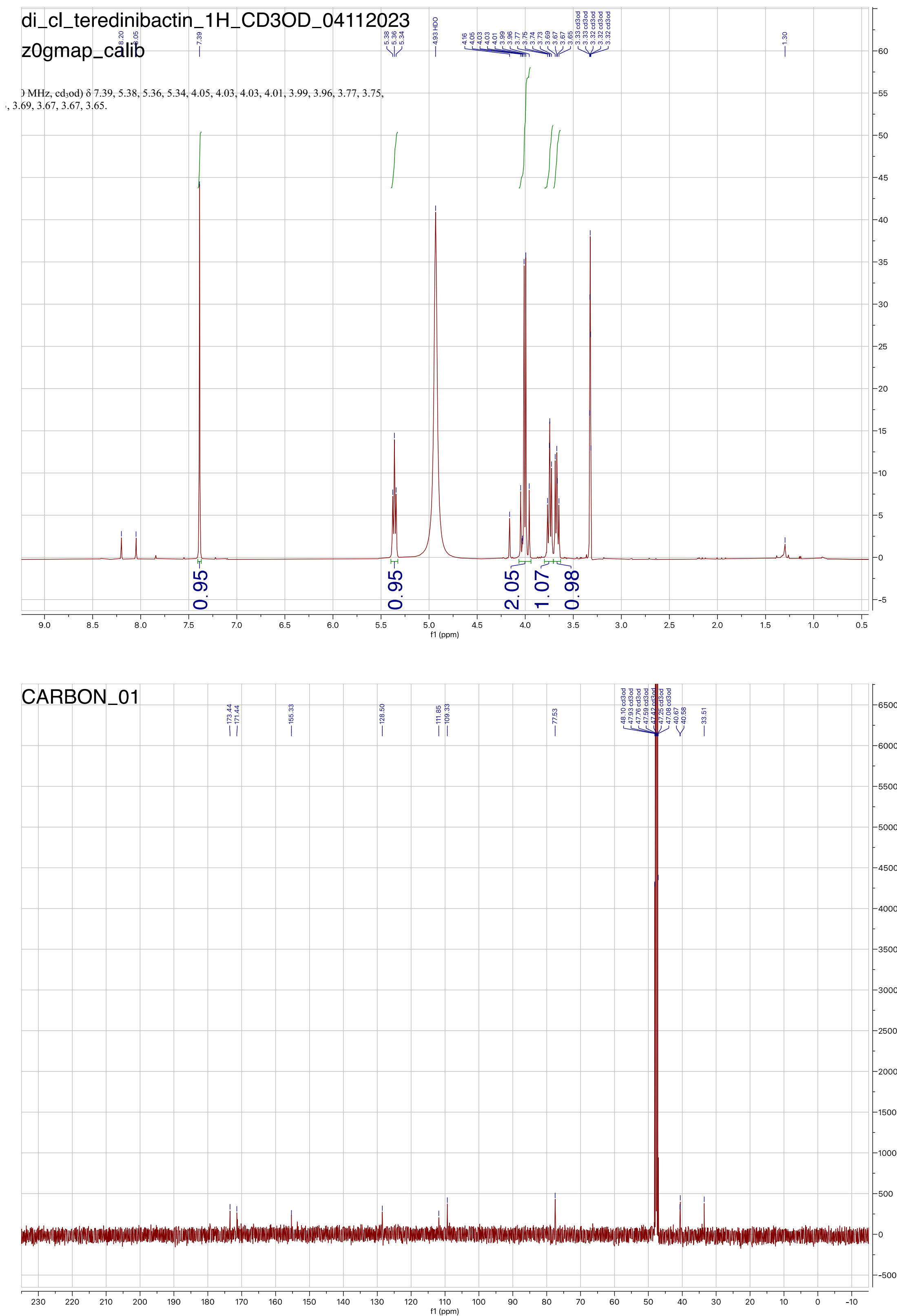

Figure S6. ^{1}H NMR and ^{13}C NMR spectra of teredinibactin analog (**5**).

https://doi.org/10.26434/chemrxiv-2024-ph6m0 **ORCID:** https://orcid.org/0000-0003-3204-3235 Content not peer-reviewed by ChemRxiv. **License:** CC BY-NC-ND 4.0

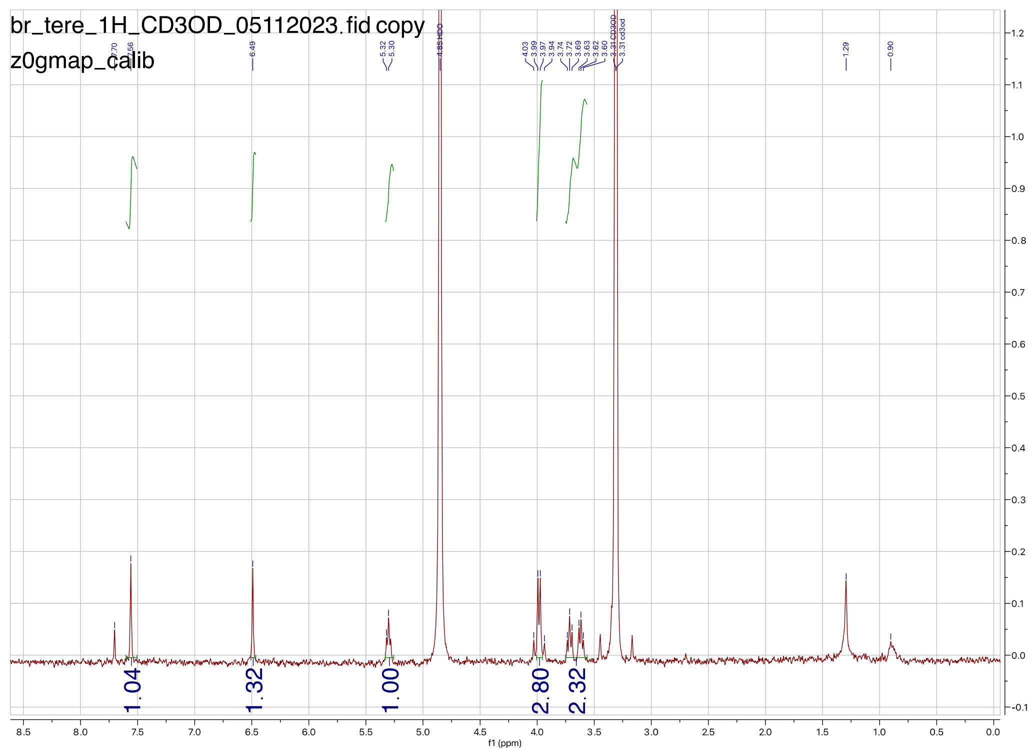

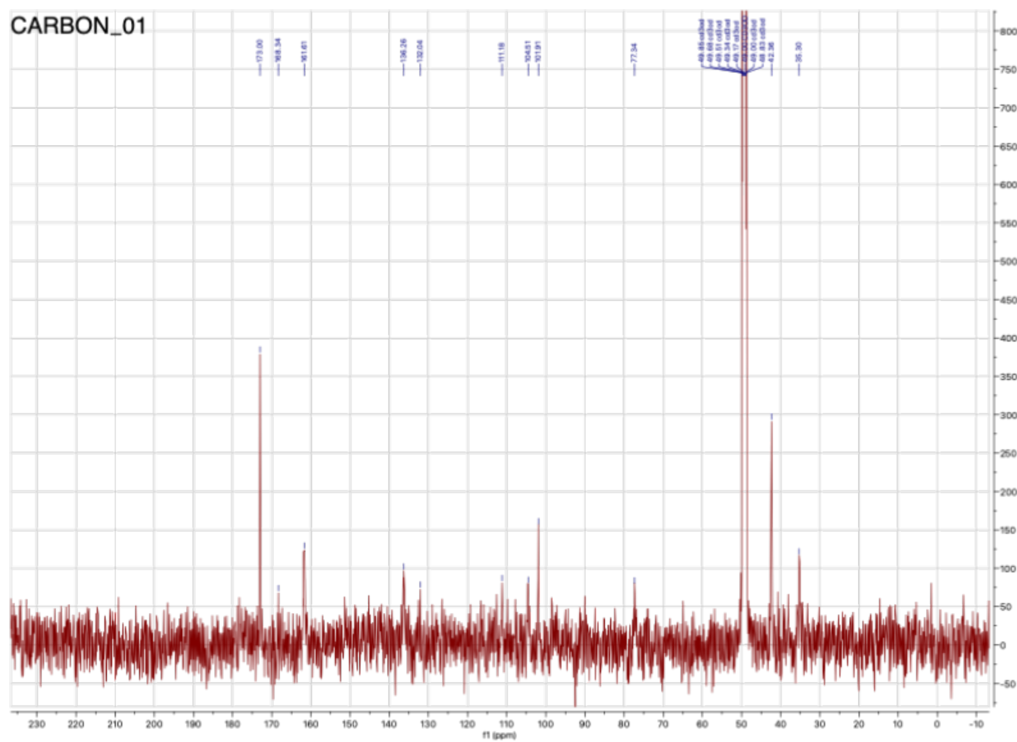

Figure S7. ^{1}H NMR and ^{13}C NMR spectrum of teredinibactin analog (**7**).

https://doi.org/10.26434/chemrxiv-2024-ph6m0 **ORCID:** https://orcid.org/0000-0003-3204-3235 Content not peer-reviewed by ChemRxiv. **License:** CC BY-NC-ND 4.0

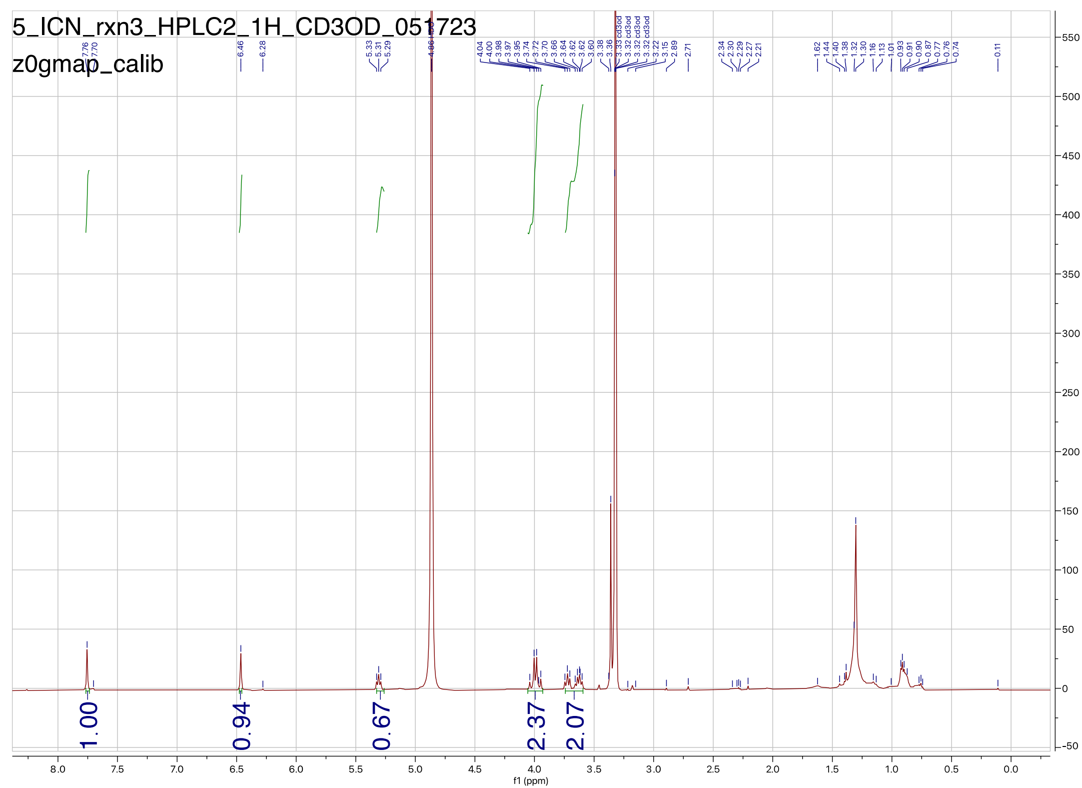

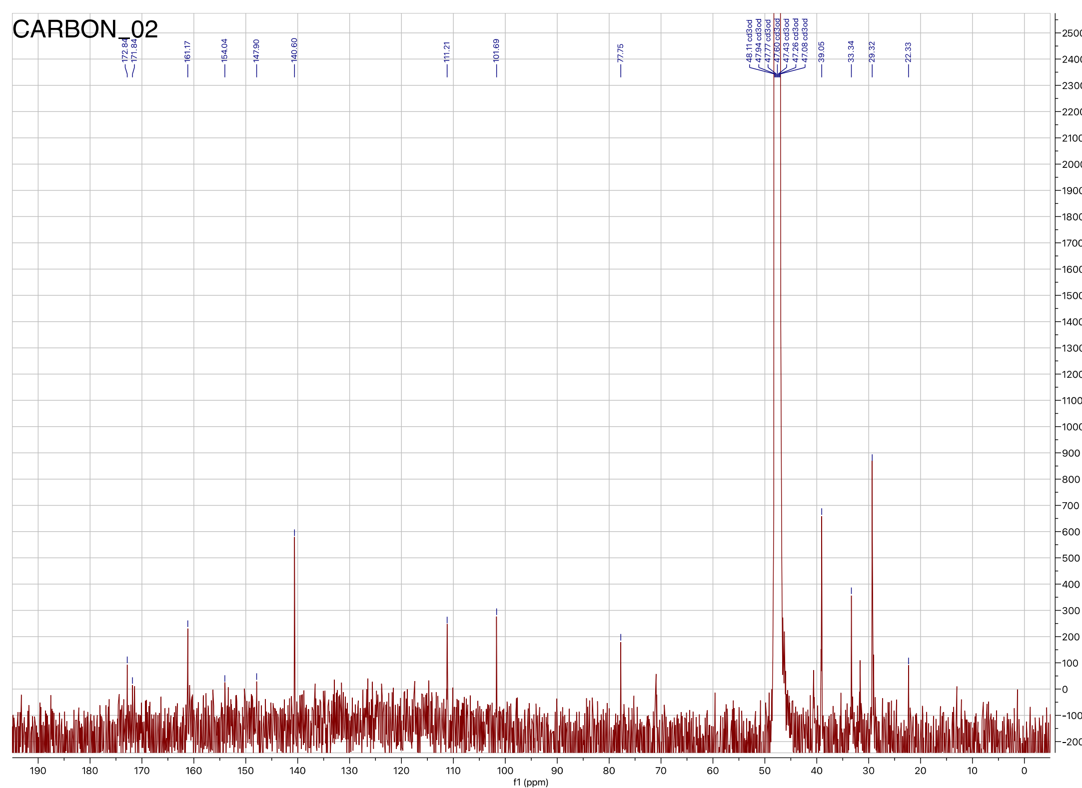

Figure S8. ^{1}H NMR and ^{13}C NMR spectra of teredinibactin analog (**10**).

https://doi.org/10.26434/chemrxiv-2024-ph6m0 **ORCID:** https://orcid.org/0000-0003-3204-3235 Content not peer-reviewed by ChemRxiv. **License:** CC BY-NC-ND 4.0

Figure S9. ^{1}H NMR and ^{13}C NMR spectra of 2,4-dihydroxybenzonitrile (**3**).

https://doi.org/10.26434/chemrxiv-2024-ph6m0 **ORCID:** https://orcid.org/0000-0003-3204-3235 Content not peer-reviewed by ChemRxiv. **License:** CC BY-NC-ND 4.0

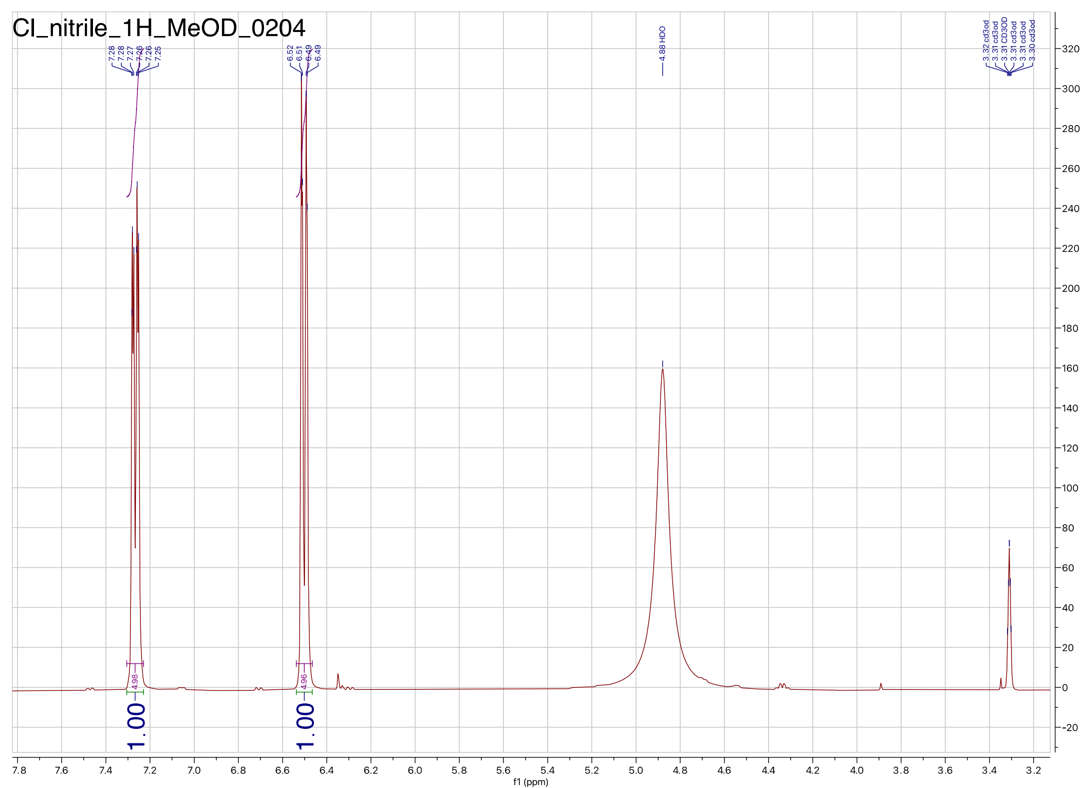

Figure S10. ^{1}H NMR spectrum of 3-chloro-2,4-dihydroxybenzonitrile (**4**).

https://doi.org/10.26434/chemrxiv-2024-ph6m0 **ORCID:** https://orcid.org/0000-0003-3204-3235 Content not peer-reviewed by ChemRxiv. **License:** CC BY-NC-ND 4.0

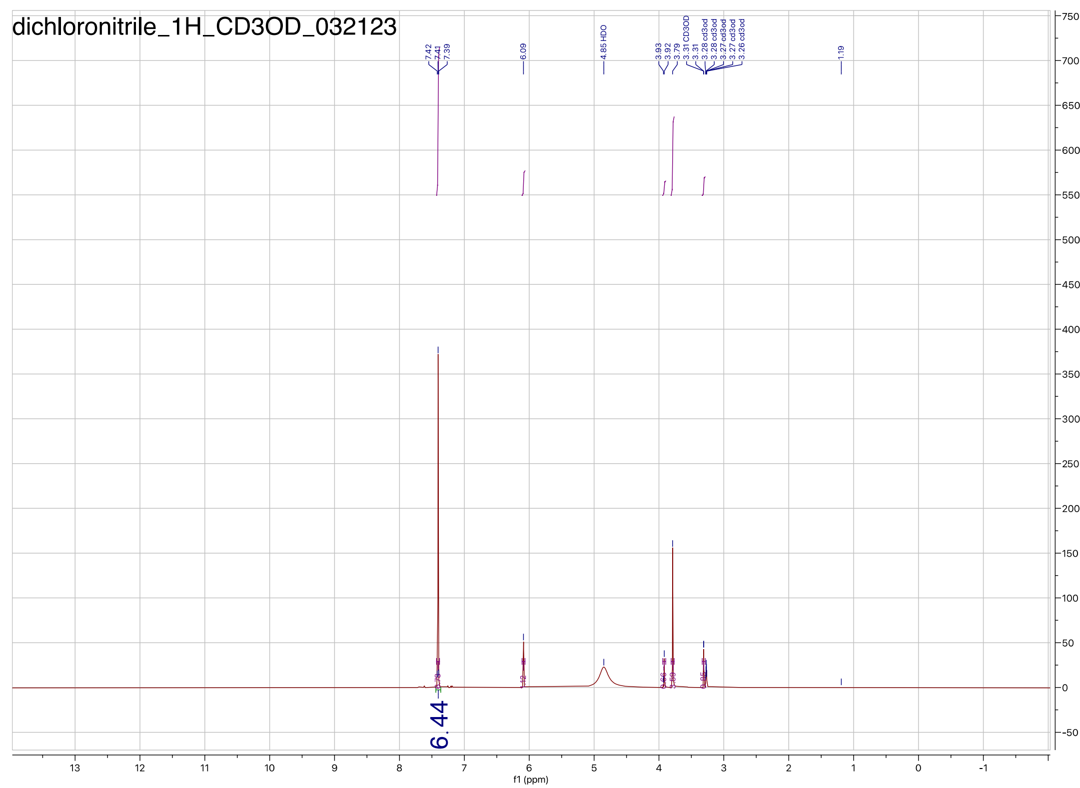

Figure S11. ^{1}H NMR spectrum of 3,5-dichloro-2,4-dihydroxybenzonitrile (**13**).

https://doi.org/10.26434/chemrxiv-2024-ph6m0 **ORCID:** https://orcid.org/0000-0003-3204-3235 Content not peer-reviewed by ChemRxiv. **License:** CC BY-NC-ND 4.0

Figure S12. ^{1}H NMR spectrum of 3-bromo-2,4-dihydroxybenzonitrile (**14**).

https://doi.org/10.26434/chemrxiv-2024-ph6m0 **ORCID:** https://orcid.org/0000-0003-3204-3235 Content not peer-reviewed by ChemRxiv. **License:** CC BY-NC-ND 4.0

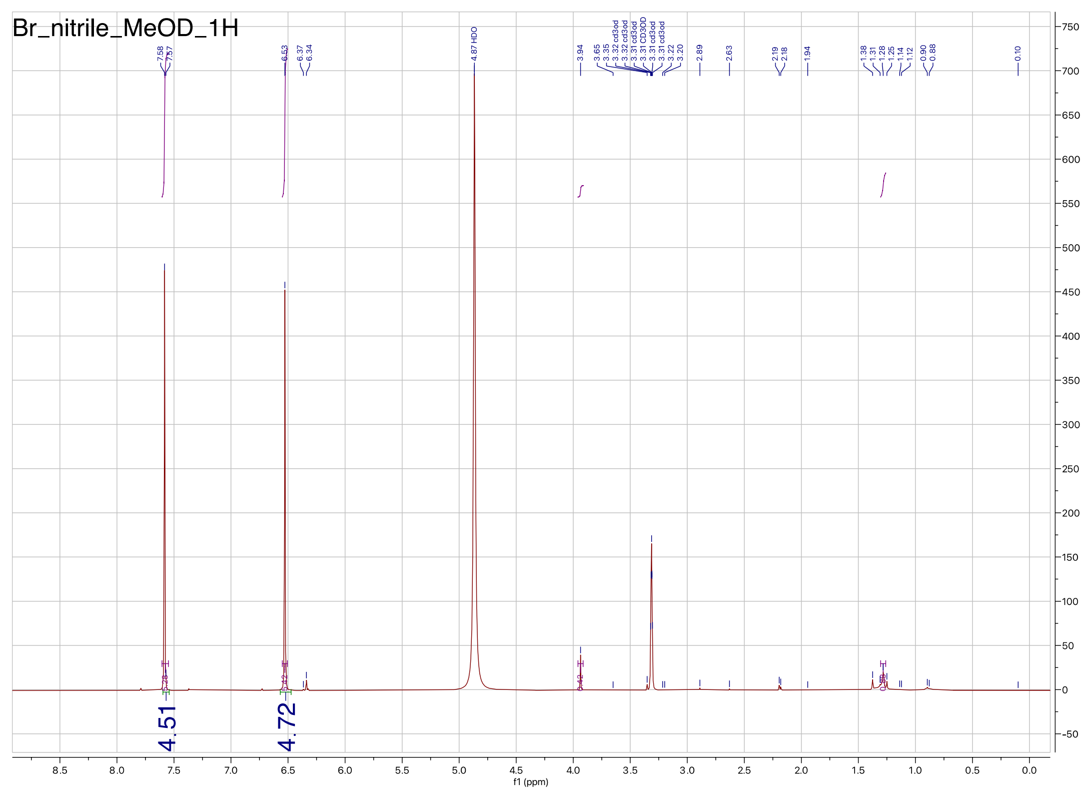

Figure S13. ^{1}H NMR spectrum of 5-bromo-2,4-dihydroxybenzonitrile (**15**).

https://doi.org/10.26434/chemrxiv-2024-ph6m0 **ORCID:** https://orcid.org/0000-0003-3204-3235 Content not peer-reviewed by ChemRxiv. **License:** CC BY-NC-ND 4.0

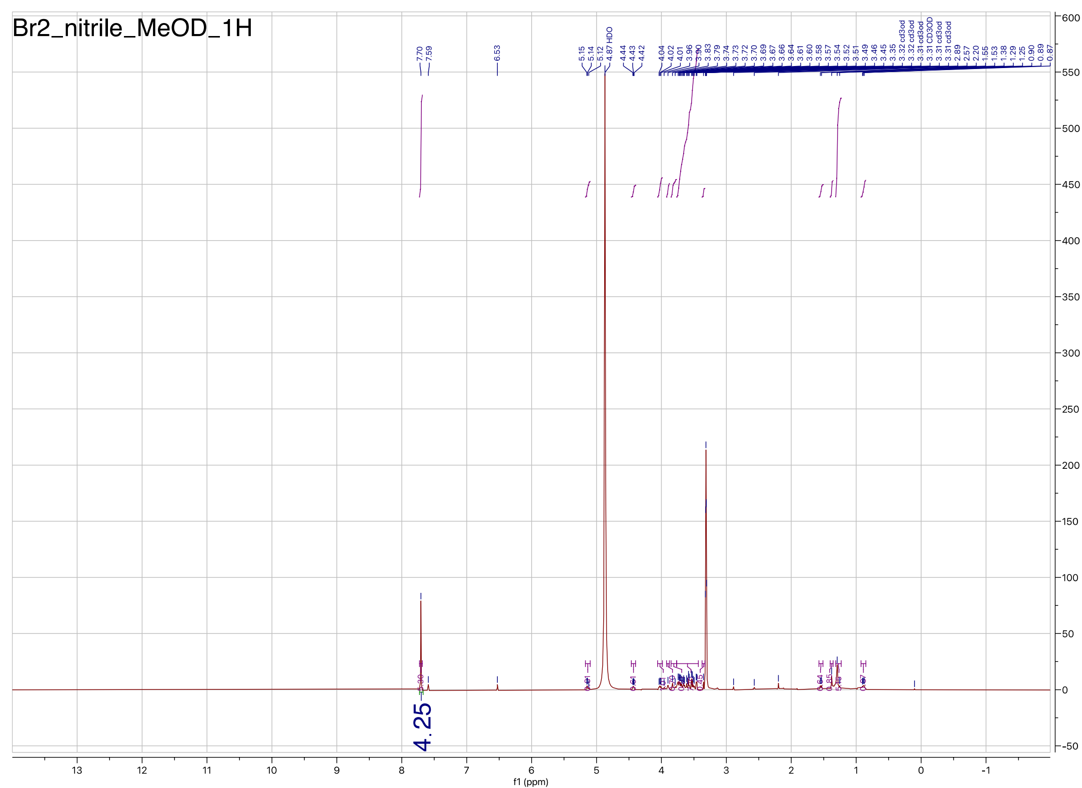

Figure S14. ^{1}H NMR spectrum of 3,5-dibromo-2,4-dihydroxybenzonitrile (**16**).

https://doi.org/10.26434/chemrxiv-2024-ph6m0 **ORCID:** https://orcid.org/0000-0003-3204-3235 Content not peer-reviewed by ChemRxiv. **License:** CC BY-NC-ND 4.0

Figure S15. ^{1}H NMR spectrum of 3-iodo-2,4-dihydroxybenzonitrile (**17**).

https://doi.org/10.26434/chemrxiv-2024-ph6m0 **ORCID:** https://orcid.org/0000-0003-3204-3235 Content not peer-reviewed by ChemRxiv. **License:** CC BY-NC-ND 4.0

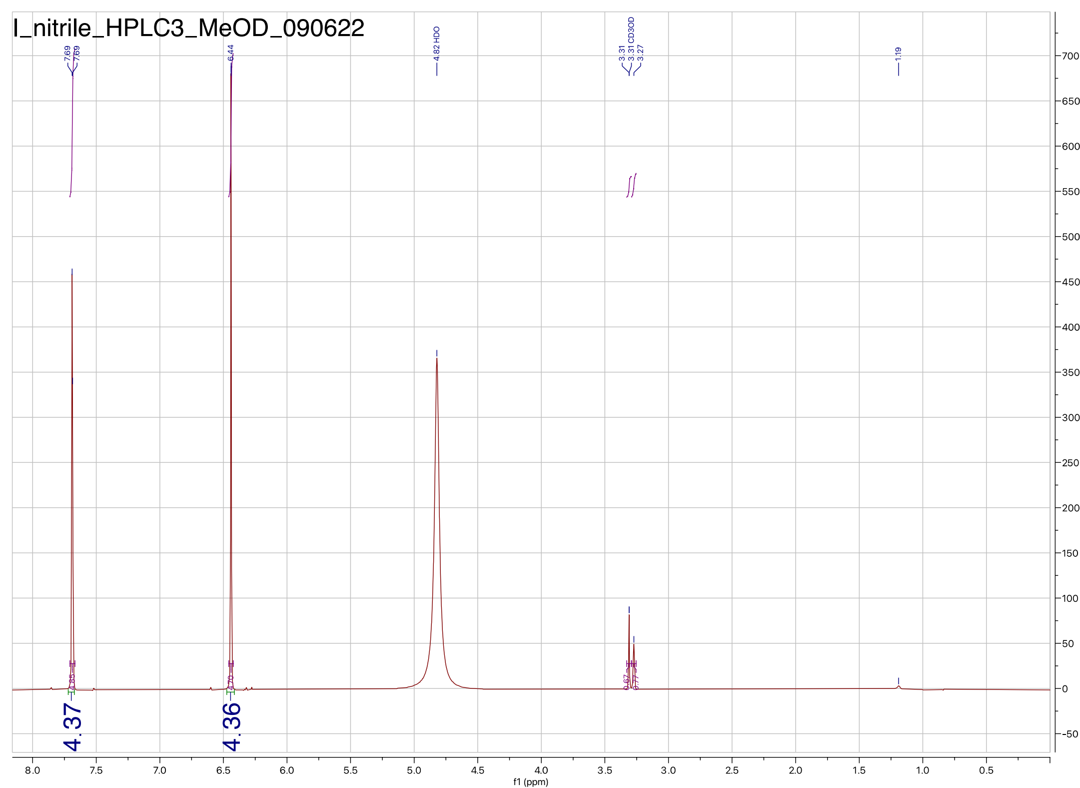

Figure S16. ^{1}H NMR spectrum of 5-iodo-2,4-dihydroxybenzonitrile (**18**).

https://doi.org/10.26434/chemrxiv-2024-ph6m0 **ORCID:** https://orcid.org/0000-0003-3204-3235 Content not peer-reviewed by ChemRxiv. **License:** CC BY-NC-ND 4.0